

**Rockslides on limestone cliffs with sub-horizontal bedding in the southwestern calcareous area, China**

Authors: Z. Feng<sup>1</sup>, Y.P. Yin<sup>2</sup>, B. Li<sup>1</sup>, K. He<sup>3</sup>

**1.** Key Laboratory of Neotectonic Movement and Geohazard of MLR at Institute of Geomechanics, Chinese Academy of Geological Science, Beijing 100081, China.

**2.** China Institute of Geo-Environment Monitoring, Beijing 100081, China

**3.** Chang'an University, Xi'an 710054, China

\*. Correspondence to: B. Li. (libin1102@163.com, +86-010-88815022)

**Abstract:** Calcareous mountainous areas are highly prone to geohazards, and rockslides play an important role in cliff retreat. This study presents three examples of failures of limestone cliffs with sub-horizontal bedding in the southwestern calcareous area of China. Field observations and numerical modeling of Yudong Escarpment, Zengzi Cliff, and Wangxia Cliff showed that pre-existing vertical joints passing through thick limestone and the alternation of competent and incompetent layers are the most significant features for rockslides. A “hard on soft” cliff made of hard rocks superimposed of soft rocks is prone to rock slump, characterized by shearing through the underlying weak strata along a curved surface and backward tilting. When a slope contains weak interlayers rather than a soft basal, a rock collapse could occur from the compression fracture and tensile split of the rock mass near the interfaces. A rock slide might shear through a hard rock mass if no discontinuities are exposed in the cliff slope, and sliding may occur along a moderately inclined rupture plane. The “toe breakout” mechanism mainly depends on the strength

characteristics of the rock mass.

**Key words:** cliff failure; sub-horizontal bedding; plane slide; toe splitting; rock slump; numerical modeling

## 1. Introduction

The southwestern calcareous area of China covers a large area of  $54.4 \times 10^3 \text{ km}^2$ , and it is highly prone to geohazards. Many multilayered carbonate rocks with sub-horizontal bedding have been deeply cut by rivers during crustal uplift and form significant topographic relief in steep slopes and cliffs. These sub-horizontal cliff slopes are usually dominated by two sets of sub-vertical conjugate joints and are characterized by slightly folded or faulted to massive rock masses. Rockslides from sub-horizontally bedded cliff failure and resulting catastrophes have occurred widely and frequently in the southwestern calcareous area of China.

Considerable research on cliff failure has been conducted in similar areas around the world(Abele, 1994; Von, 2002; Rohn, 2004; Embleton, 2007; Ruff, et al., 2008; Palma, et al., 2012), such as the North Calcareous Alps in Austria. It is believed that water, lithology, geological structure, and karstification are of primary importance in triggering rockslides from cliff failure (Kay, et al., 2006). These factors dominate the tearing and shearing failure mechanism of the rock masses and joints, which are directly displayed in the consequent failure behavior of the cliff slopes. Types of rockslides with different detachment mechanisms (slumps, plane slides, topples, and lateral spreading) in sub-horizontally bedded cliffs with particular geological settings and triggering mechanisms have been described by engineering geologists, e.g., the collapse of the Mt. Sandling and Mt. Raschberg limestone towers had a complex failure sequence from lateral spread to

toppling followed by rock fall (Rohn, et al., 2004). In addition to lateral spreading, a cliff slope with a geological formation of hard rock on a soft base may undergo the translational sliding or slumping of slab-shaped blocks (Poisel, 2005). In addition, the karst process is an inevitable factor in rockslide formation. Tectonic joints keep widening and extending to the deep of rock mass by constant dissolution and disgregation of underground water, forming boundaries of perilous rocks (Santo, et al., 2007). It is believe that karst plays an important role in rockslides from carbonate mountains, especially for gently bedding-inclined slopes which are unfavorable to failure.

Active underground mining is widespread in the southwestern calcareous area of China. There is the potential for damage to cliff faces and overhangs when mining activity occurs beneath cliffs. This has been repeatedly shown to be true. Taking the Southern Coalfields of Australia as an example, several types of cliff failure have been witnessed in the goaf area, although no instabilities have been reported beyond the mining area (Kay, 2006). However, there is no available and widely accepted model that can predict the failure susceptibility of steep slopes close to mining. This is because of the complex interaction of factors influencing the stability of steep slopes, which include geometry, geology, geological structure, environmental factors, and technical mining parameters. An integrated method combining landslide science and mining subsidence science is promising as a direction for future research.

This study focuses on the failure mechanisms of cliffs with sub-horizontal bedding in the southwestern calcareous area of China and the recognition of these features in field investigations. The three cases presented occurred during the last 10 years and caused great damage to both human life and assets. Furthermore, post-failure behavior, such as rock avalanches and debris flows, is not included in descriptions of failure mechanisms of steep slopes. The term “failure

mechanism” in this study particularly refers to the detachment mechanism of rock masses from the cliff slope.

## **2. Geological background**

According to the Geo-hazards Survey Plan launched by Ministry of Land and Resources of China since 1999, most of the counties and cities in the southwestern calcareous China are most serious area suffering from geo-hazards (Zhang et al, 2000; Li et al, 2004). The likelihood of rockslide instability in the area is high, mainly because of the local geological evolution. Tectonic movement during the Mesozoic was characterized by compression and formed the area into a fold belt, mainly striking NNE (Fig.1). Neotectonic uplift raised the thick carbonate rocks to high altitude and shaped the steep and folded landforms.

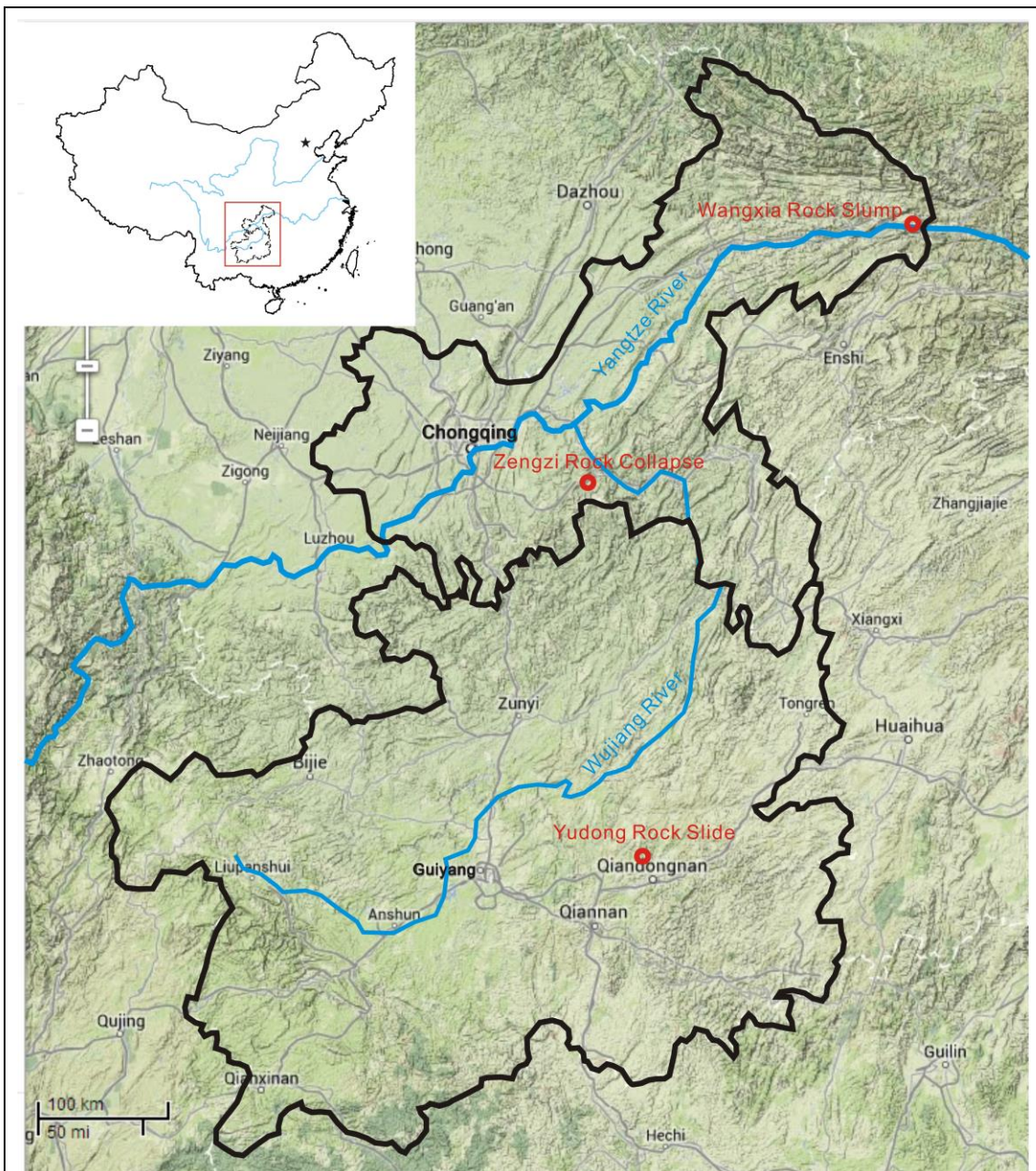


Fig. 1 Locations of three rockslides: Wangxia Rock Slump, Zengzi Rock Collapse, and Yudong Rock Slide.

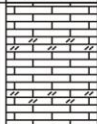
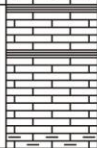
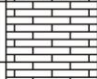

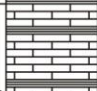
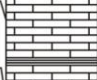
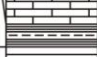

System	Series	Symbl	Column	Thickness	Lithology
Triassic	Lower	$T_1^2$		520~650m	layered limestone and dolomite, usually in cliff landform.
		$T_1^1$		660~680m	mudstone, layered limestone, dolomitic limestone, locally contains shale bands.
Permian	Upper	$P_3^2$		95~134m	layered limestone, usually be shaped into cliffs.
		$P_3^1$		98~143m	layered to blocky limestone rock, underlain by a measure of claystone, shale, and coal seams
	Middle	$P_2^3$		203~377m	layered to blocky limestone rock, interbedded with carbonaceous shale, usually cut by conjugate joints and in cliff landform.
		$P_2^2$		47~106m	thick layered limestone, interbedded with argillaceous bands, usually cut by joints and in cliff landform.
		$P_2^1$		2~13m	claystone, carbonaceous shale, interbedded with coal seams, bauxite, shaped into steep slope under the hard cap rocks
Silurian	Middle	$S_2$		500~680m	shale, silty shale, easily weathered and usually in a landform of gentle slopes

Fig.2 The most common outcrop sequence in southwest calcareous China

78

79 Many layers of carbonate rocks were deposited from Permian until Triassic time, and were  
80 interbedded with weak planes or soft strata (Fig.2). The carbonate rock masses possess great  
81 strength and integrity; thus, they usually form steep slopes hundreds of meters high, e.g., the Three  
82 Gorges, if there are no intercalated soft strata. Under these circumstances, slope movement is  
83 mainly controlled by discontinuities such as weak interlayers, karst, and fissures. The thick  
84 carbonate succession in the southwestern calcareous area of China contains multiple layers of  
85 weak shale planes, including carbonaceous shale and pyrobituminous shale. The strength of the  
86 shale planes is relatively low and significantly varies with the weathering process, from virgin  
87 rock to fractured planes to argillaceous layers. The strength of carbonaceous shale sandwiched in  
88 the  $P_1$  limestone at Lianziya Cliff is low that the cohesion and internal friction angle are 0.08–0.39  
89 MPa,  $18^\circ$ – $21^\circ$  and 0.06–0.078 MPa,  $18^\circ$ – $19.8^\circ$  for dry and saturated samples, respectively (Ding,

et al. 1990). The weak interlayers play a significant role in mass movement. When soft strata underlie hard rock, the yielding of the soft base may cause the uneven subsidence of the cap rock. Lateral spreading and slumps with backward tilting are caused by this type of destabilization mechanism, in which failure propagates uphill.

In the southwestern calcareous area of China, coal measures are common soft strata, accompanied by thick carbonate sequences. Except for coal seams, the coal measures are usually composed of associated interlayers of shale, carbonaceous shale, pyrobituminous shale, and bauxitic claystone.

Mining is active in these coal measures using the techniques of room and pillar mining and longwall mining. The depth of cover ranges from dozens to hundreds of meters. It is believed that underground mining activities can change the engineering geological conditions and reduce the stability of cliffs (Tang, 2009; Altun, et al., 2010; Marschalko, et al., 2012; Lollino, et al., 2013), . Cliff failures and the resulting catastrophes, examples of which are discussed below, are related to underground mining.

Karstification is a significant factor when discussing the reasons for carbonate slope failure. It particularly affects steeply inclined faults and tectonic joints and slowly widens the discontinuities to create large open fractures, which foster rockslides (Santo et al., 2007; Parise, 2008). In addition, the karstification process can cause a significant reduction in the mechanical properties of the carbonate rock mass. This is very important for toe-constrained slides, which depend on the strength of the rock mass at the toe. In some cases, the underground karst voids play the same role as goaf, and cavern breakdown may also lead to landslides (White, et al., 1969; Parise, 2010).



### 3. Failure modes

Different types of rockslides have been observed in thickly and sub-horizontally bedded limestone escarpments. Gently inclined bedding is unfavorable for large translational slides. Slope failures, including slide, collapse and slump, are discussed below in detail to explain their mechanisms. Three examples are given: the Yudong Escarpment, Zengzi Cliff, and Wangxia Cliff (Fig. 1).

#### 3.1 Rock slide at the Yudong Escarpment

On February 18, 2013, a rock slide occurred in Longchang County, Guizhou Province. The mass movement is located in a high and steep bank of the Yudong River, close to an underground mining area (Fig. 3). The S308 provincial road runs on the opposite bank of the river. The rock slide buried several houses and five people beneath the escarpment and blocked the river.

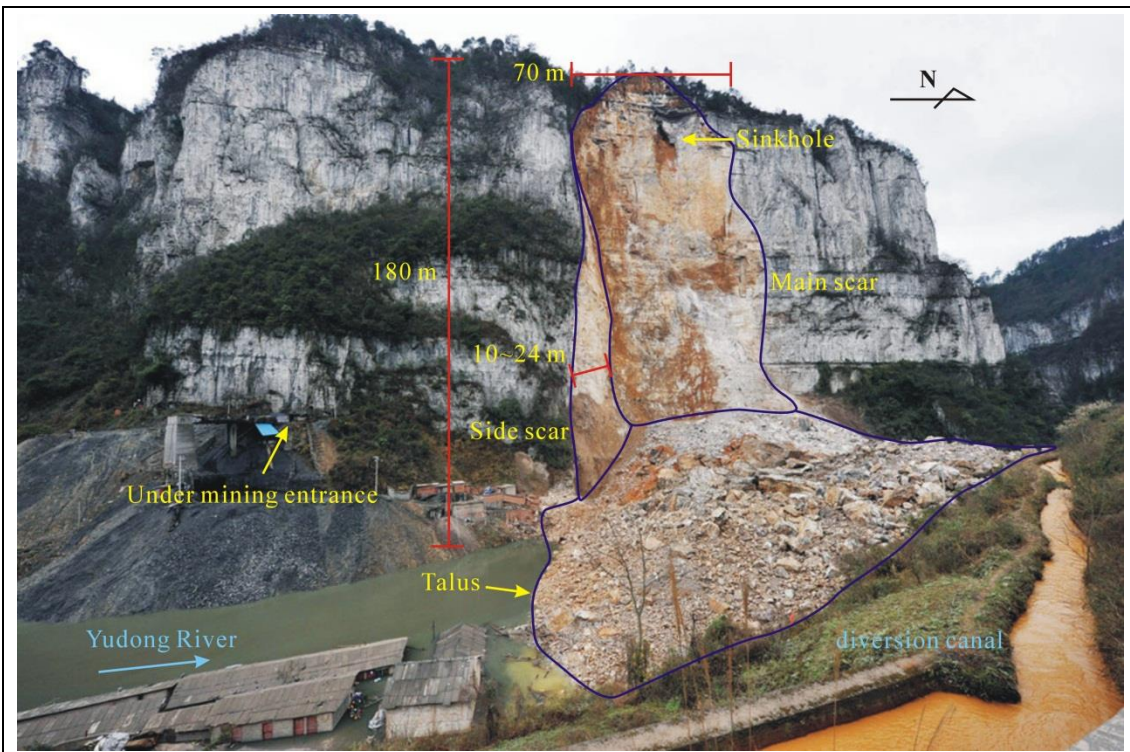


Fig.3 Photograph showing an overview of Yudong rock slide I.

The Yudong Escarpment is about 220 m high and the slope angle is more than 80°. The steep



slope faces in the direction SE100°–130°, and the dip direction is NW325°, with slightly inclined bedding. The outcrop consists of thickly bedded  $P_2^2$  limestone and underlying  $P_2^1$  coal measures. The Yudong Escarpment lies in the gentle eastern flank of the Yudong Syncline, which strikes NNE. As a result, a set of NNE-trending joints and a conjugate set of NW-trending joints are present in the rock mass. The orthogonal 130°/70° and 80°/75° joints cut the 325°/9° rock beds into prism- and tower-shaped blocks on the edge of the cliff. The jointed limestone is moderately weathered, and the uniaxial compression strength of intact rock reaches 30 MPa. The coal measures are composed of thickly bedded argillaceous shale and coal seams. Coal extraction has been active in the soft basal unit, and the goaf is about 200 m deep behind the cliff face. The “2.18” Yudong rock slide originates from one of these unstable blocks with a volume of about  $30 \times 10^4 \text{ m}^3$ . Several types of karst are observed in the rock slide area, including sinkholes, karst tunnels, and dissolution fissures. A remote sensing image taken the day after the rock collapse shows a sinkhole at the crest with a diameter of 2.2 m immediately behind the fall. The pipe flow in the tunnels and cracks induce static and dynamic pressure, acting on the unstable rock block and changing the stability. However, because of abundant vegetation, the sinkhole is not visible in a previous image that was taken in the summer of 2012 (Fig. 4). The intense karstic erosion of a yellowish-orange color has been observed on the vertical scar. The selective karst widens and connects the pre-existing steep joints so that the area of the rock bridge covers less than 30% of the main scar (Huang, 2013). The directed scratches indicate the brittle failure of the rock bridges and consequent fall of the rock mass. The rock slide left two scars originate from joints. The main scar is nearly parallel to the cliff face and about 80 m wide. The upper part of the main scar is a sub-vertical plane, and the lower parts are planar and dip out of the cliff. The conjugate side scar is



154 failure of the rock mass in the toe area can be explained by the brittle failure of the rock mass  
155 under uniaxial compression tests. In other words, it is largely dependent on the mechanical  
156 properties of the rock mass at the toe. The toe is sheared along random discontinuities of limited  
157 persistence traced by the rupture surface (Fig. 7).

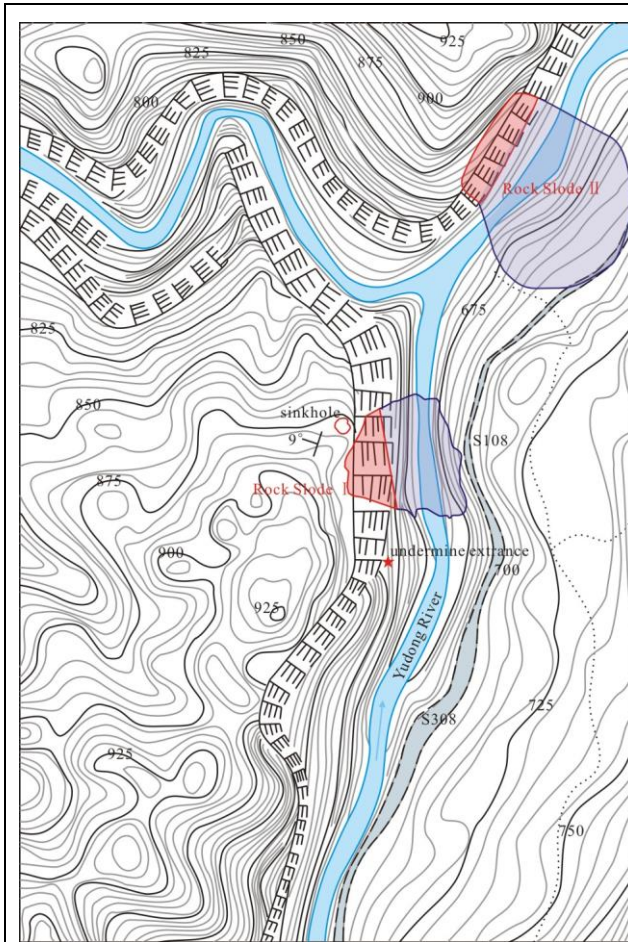


Fig. 5 Rock slide II is located north of rock slide I and has the same geological conditions, except for undermining. The volume of the talus of rock slide II is  $30 \times 10^4 \text{ m}^3$ . It blocked the Yudong River and covered 80 m of the S308 road.

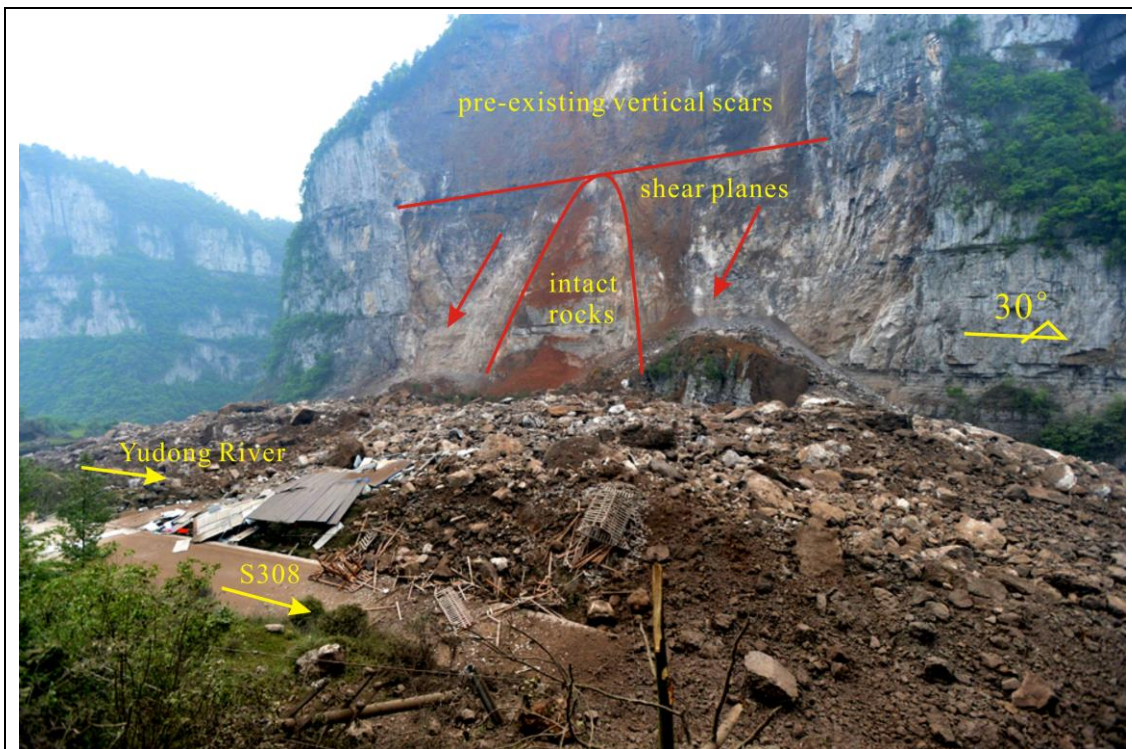


Fig. 6 Photograph showing rock slide II at Yudong. The pre-existing vertical scars are coated with karst of a yellowish-brown color, while the rupture surfaces are white and gray, indicating brittle failure and planar sliding through the limestone.



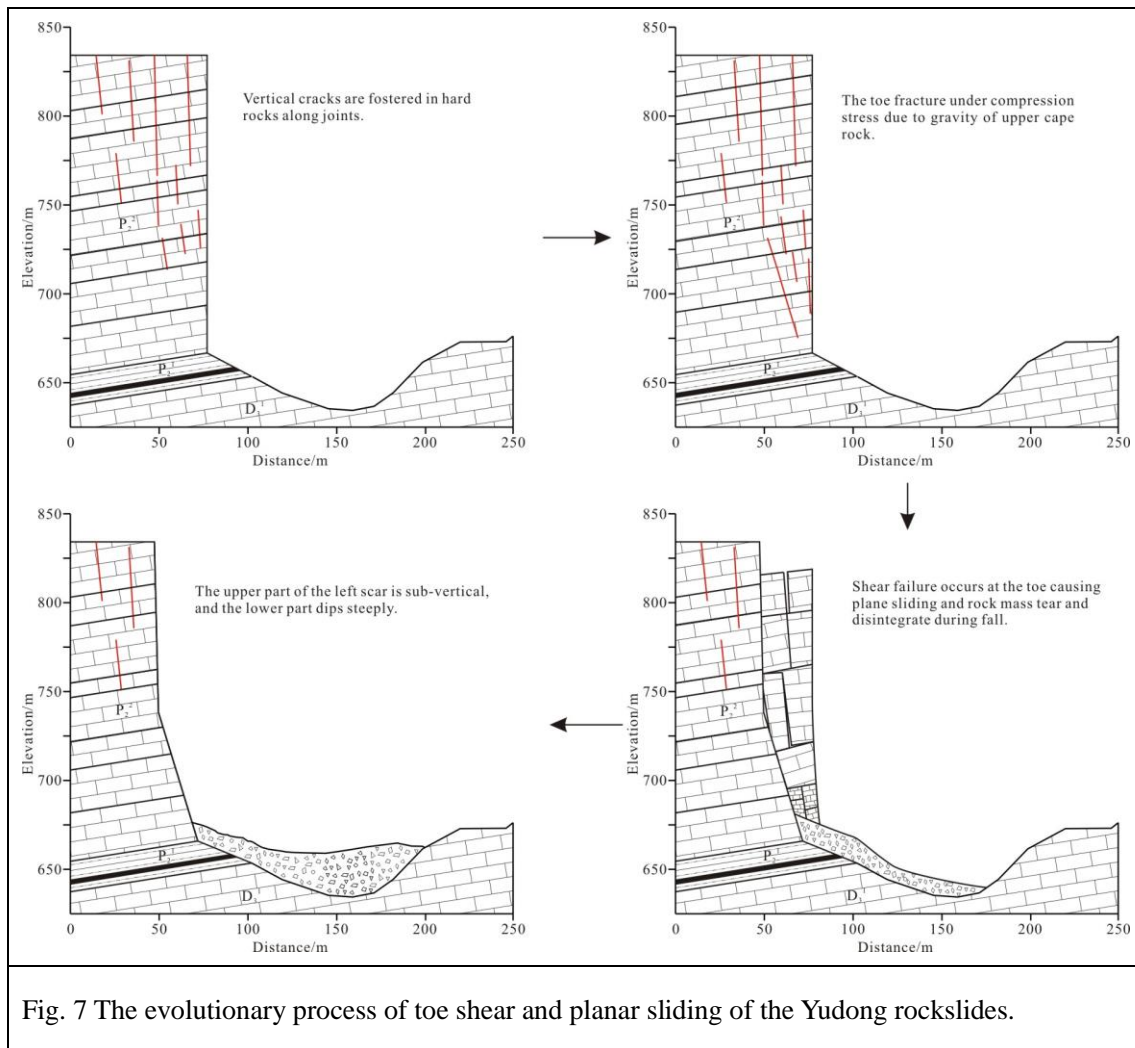


Fig. 7 The evolutionary process of toe shear and planar sliding of the Yudong rockslides.

158

### 159 3.2 Rock collapse at Zengzi Cliff

160 Zengzi Cliff lies in the gentle and wide core of the Jinfo Mountain Syncline, Nanchuan County  
 161 of Chongqing, in a “hard on soft” landform. The vertical limestone consists of two platforms  
 162 separated by softer rock (Fig. 8). Two major tectonic joints in the hard rocks strike at  $N40^{\circ}-50^{\circ}E$   
 163 and  $N30^{\circ}-50^{\circ}W$ , with dip angles of  $70^{\circ}-88^{\circ}$ . These two sets of joints are approximately  
 164 orthogonal to each other and perpendicular to bedding. The bedding trends at  $300^{\circ}-305^{\circ}$  with a  
 165 very low inclination ( $4^{\circ}-7^{\circ}$ ). The upper platform is U in shape; hence, the steep slope varies from  
 166 anacinal to plagioclinal and cataclinal in different parts of the edge. Beneath the cliff,  $S_2$  silty  
 167 shale forms a soft base and a gentle slope ( $20^{\circ}-30^{\circ}$ ). Talus occurs everywhere under the cliffs,

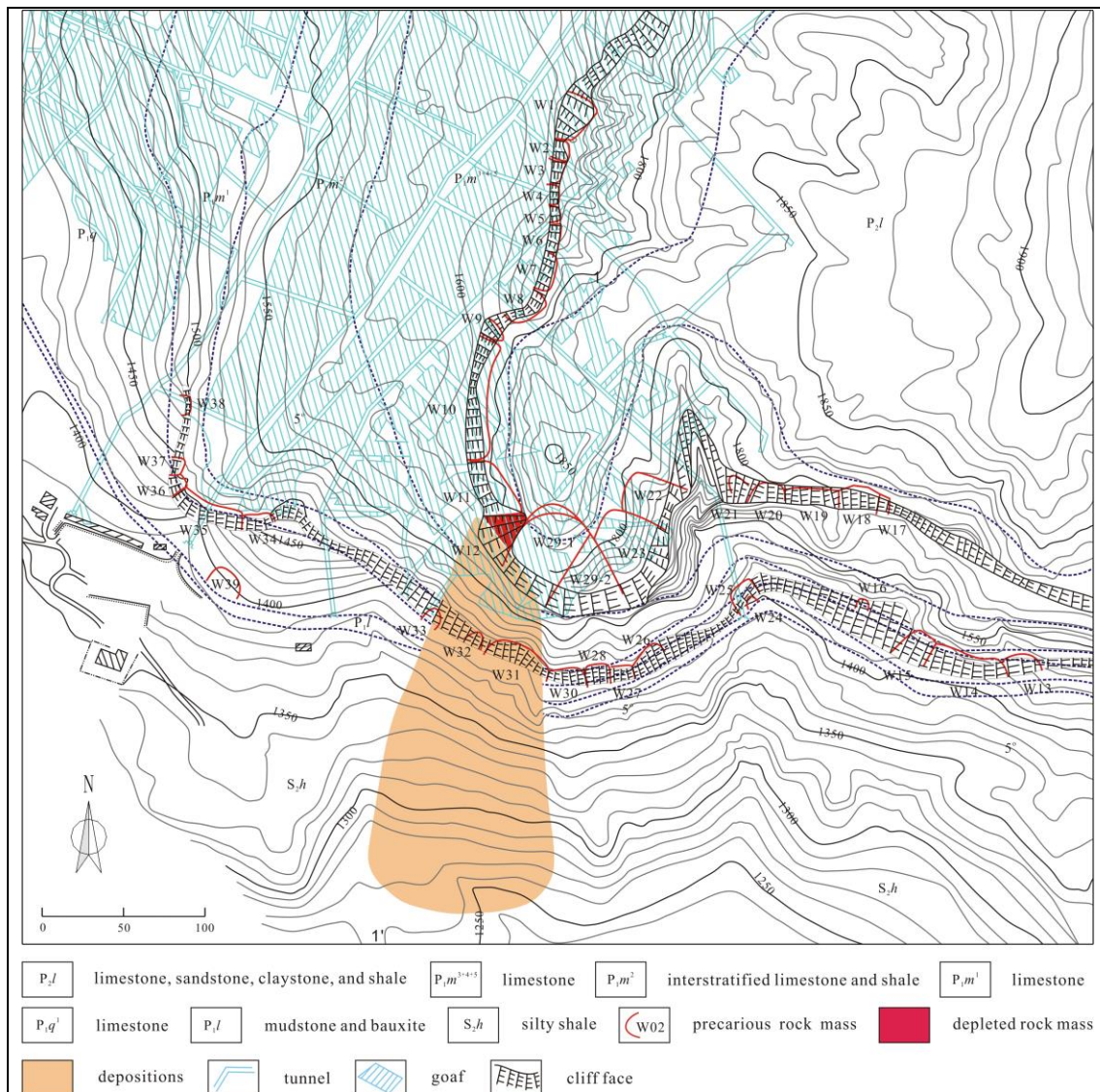


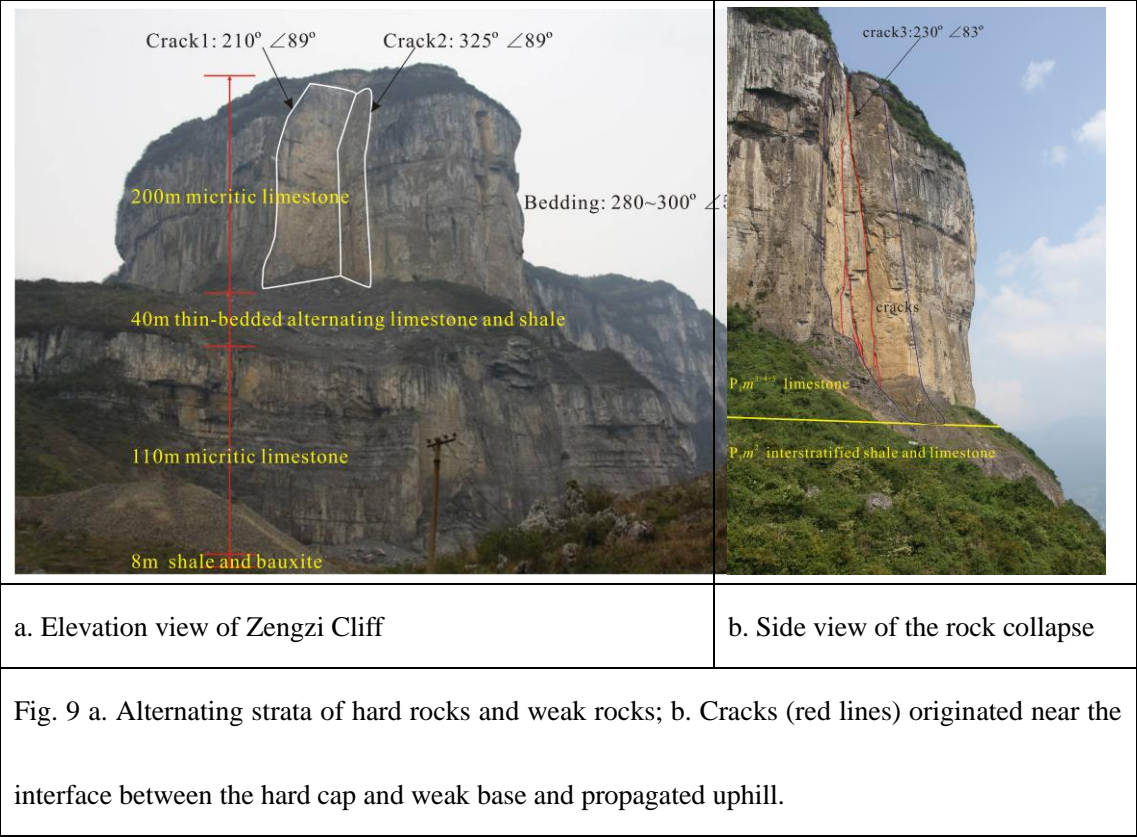
Fig. 8 Topographic map of the Zengzi Cliff area and the distribution of precarious rock masses on its edge. Room and pillar mining has been conducted in the P<sub>1</sub>*l* sequence since 1983, and the goaf extends from south to north. The depth of the goaf is about 100–120 m for the first step and 350–400 m for the second step.

169

Rocks frequently fall in the Zengzi Cliff area. On August 12, 2004, a massive rock collapse occurred in the upper platform, which is about 200 m high (Fig. 9). The depleted mass is a prism block shaped by sub-vertical joints and bedding. Two vertical back scars and a groove surface in



173 the underlain soft strata are exposed after the collapse. Large areas of the scars are coated with  
 174 karst argillaceous fillings and yellowish-orange calcite, while the rock bridge failure scars are  
 175 fresh. Field investigations showed that the head scars are wide open prior to the massive collapse.  
 176 Seepage forces and frost from percolating water acted on the prism block over a long time and  
 177 influenced the stability; however, only karst could alter the conditions in the rock adjoining the  
 178 slope by increasing the connectivity of back scars. The underlying soft strata consist of alternating  
 179 beds of thin-bedded shale and medium-bedded limestone, and as a result of weathering, form a  
 180 40-m-high slope.



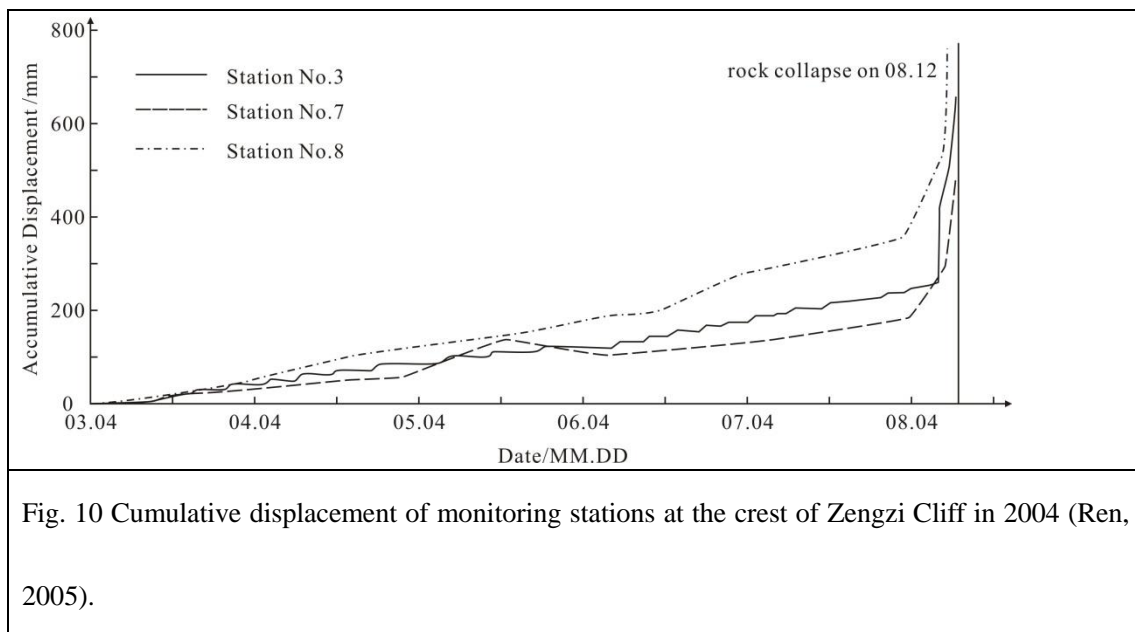
181

182 Mining activity has been conducted for decades, but community monitoring started in 2001.

183 The opening velocity of the head scar was very slow from 2001 to 2003 (Ren, 2005). It increased

184 to 4–15 mm/10 d in the period between April and July 2004 (Fig. 10), and signs of pre-collapse,

(rock falls) were repeatedly observed. At that time, the government issued warnings and evacuated residents and workers. The velocity abruptly increased from August 10, and the increment reached 658 mm on the last day. The process of the Zengzi rock collapse was captured on video: the tower dropped vertically and disintegrated while falling. It is unusual that the failure initiated in the bottom of the hard block rather than the underlying soft strata. The splitting of the hard rock mass at the toe led to tower collapse. The curved surface in the soft strata will have been carved by collision.



Tensile splitting has been observed in uniaxial compression tests of rock samples with high brittleness and strength, such as limestone. There are several reasons why the collapse did not start with shear failure in the underlying strata. The rock mass in the bottom of the tower block is in poor condition: fractured and weathered. Drill cores obtained strongly karstic rock containing dissolution pores, caves, tufa, and calcite. The drilling also revealed at least 11 fissures, some of which were filled with yellow clay (107 Geology Team, 1995). This is because the underlying strata are low-permeability soft rocks; hence, there are steady water flows immediately above.

Furthermore, the soft strata are not sufficiently weak. These strata consist of interbedded thin layers of shale (0.1–0.2 m) and medium-thick limestone. The tower block could easily shear through the shale but not the intercalated limestone. Under these circumstances, tensile split failure of the tower bottom is a reasonable failure mechanism, involving compression fracturing and horizontal shearing in the shale beds (Fig. 11). Field studies and deformability tests on rock masses all around the world have demonstrated that folded and flat-lying rock masses are prone to tensile splitting near thin weak planes. Compression fracturing and tensile splitting are important failure mechanisms for sub-horizontally bedded slopes. The Zengzi cliff collapse exposed back scars in the nearby deformable rock mass, which propagated uphill (Fig. 9b), and a fractured rock mass was observed near the shale interface.

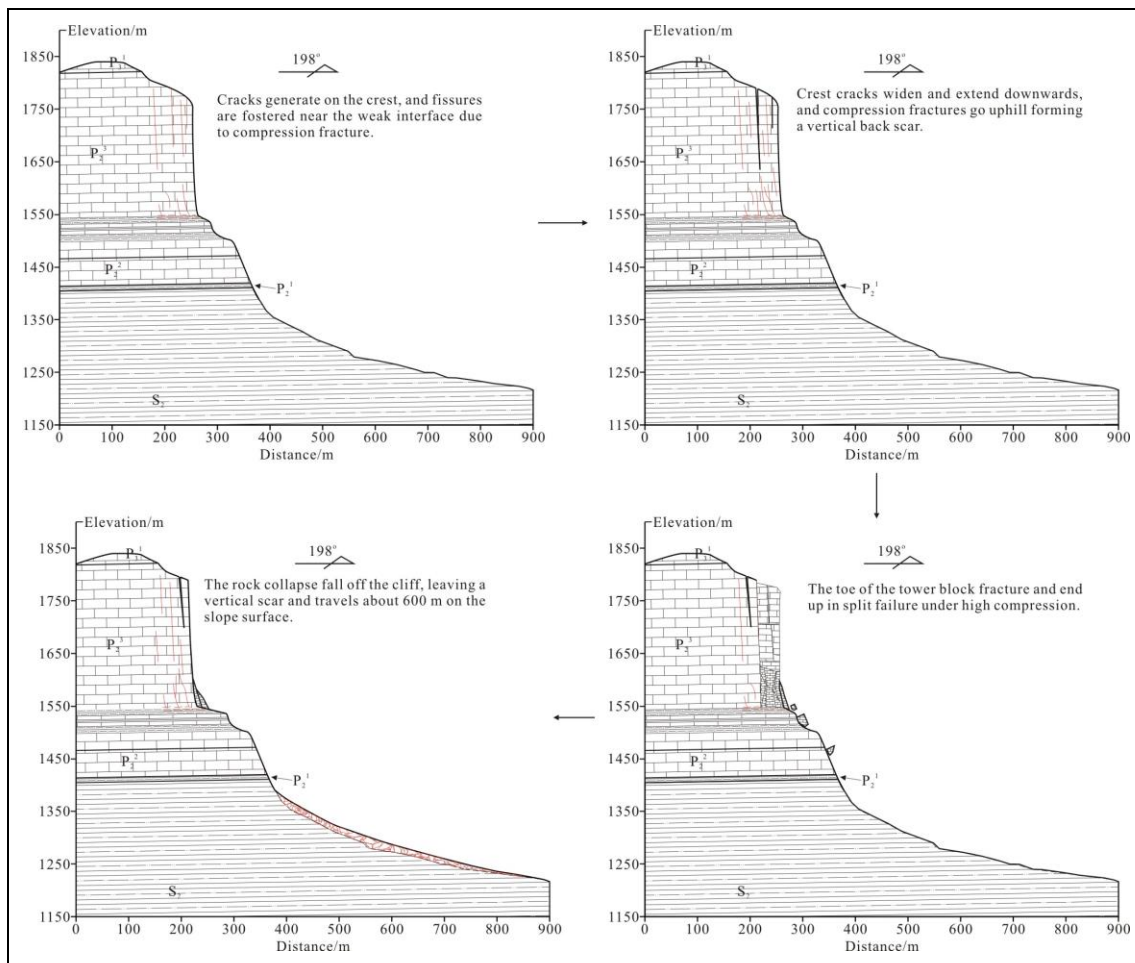


Fig. 11 Failure process of the Zengzi rock collapse, involving toe splitting and tensile failure.

### 3.3 Rock slump at Wangxia Cliff

When the base is sufficiently weak, and there is a steep fracture separating the column from the slope in the cap area, a rock slump with back-tilting mechanism is likely to occur. The Wangxia Cliff failure slump mechanism involved isolated limestone block breaking through shale at the toe, with rotational movement. The Wangxia Cliff is situated at the top of the left bank of the Yangtze River in Wushan County of Chongqing, about 1000 m above the water level (Fig. 12). Located in the flat core of the Hengshixi Fold, the bedding is slightly inclined ( $3^{\circ}$ – $8^{\circ}$ ) and strikes at  $335^{\circ}$ – $340^{\circ}$ , opposite to the cliff face. Interbedded shales, mudstones, and coal seams form a gentle slope and separate the  $P_3$  limestone into two cliff steps. A country road passes over the slope below the 70–75-m high limestone escarpment, which contains several isolated slab- and prism-shaped blocks. On October 21, 2010, a prism with a volume of  $7 \times 10^4 \text{ m}^3$  became a rock slump failure.



Fig. 12 Overview of Wangxia Cliff prior to the catastrophic rock slump. G01 represents a GPS station, and Lw02–Lw07 indicate the displacement monitoring stations. The rock slump of October 21, 2010 was controlled by vertical scars T11 and T12. The red lines represent fissures in the rock mass.

223

224 The slope movement can be traced back to June 18, 1999. Four collapsecraters and nine cracks

225 were observed in the crest area after 108.5 mm of rainfall on June 15 and 16 (Le, et al., 2011).

226 Intensive deformation began on August 21, 2010, after four days of concentrated rainfall.

227 Repeated pre-collapse signs were observed. Crown cracks widened, and new cracks occurred on

228 the crest. Rocks fell off from the cliff face and vertical scars in the rock mass. In addition, gravelly

229 soils flowed out from steep cracks at the toe. Transverse ridges and cracks were observed on the

230 country road beneath. The mass movement accelerated as a result of 70 mm of precipitation from

231 October 10 to 13. The fissures in the isolated blocks extended and widened. Rock falls became

more obvious both in volume and frequency. Finally, a massive rock slump occurred on October 21, in which the isolated prism slid downhill, breaking through the toe and leaning against the back scars. The underlying weak rocks were squeezed out and scattered over the slope surface. Displacement monitoring showed that the crest was dominated by subsidence, while the horizontal and vertical displacements were about the same at the base (Fig.13). The incompetent base showed horizontal movement and little subsidence. These phenomena were caused by ductile yielding and rotational shearing in the incompetent base (Fig. 14). The squeezing out contributed to the uphill propagation of cracks and disintegration of the mountain into slab- and prism-like blocks.

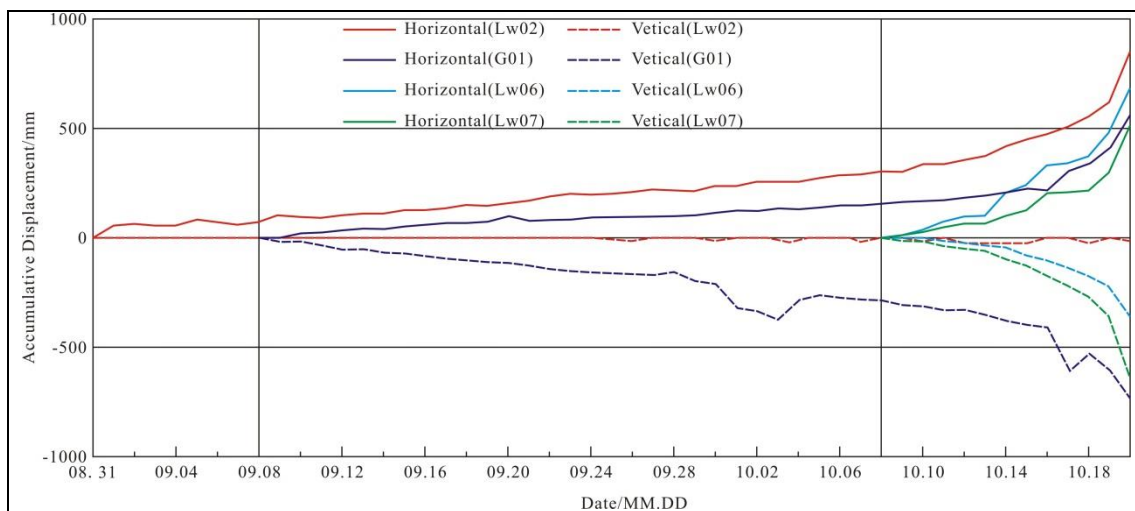


Fig. 13 Cumulative displacement at monitoring stations at the Wangxia rock slump (Le, et al., 2011).



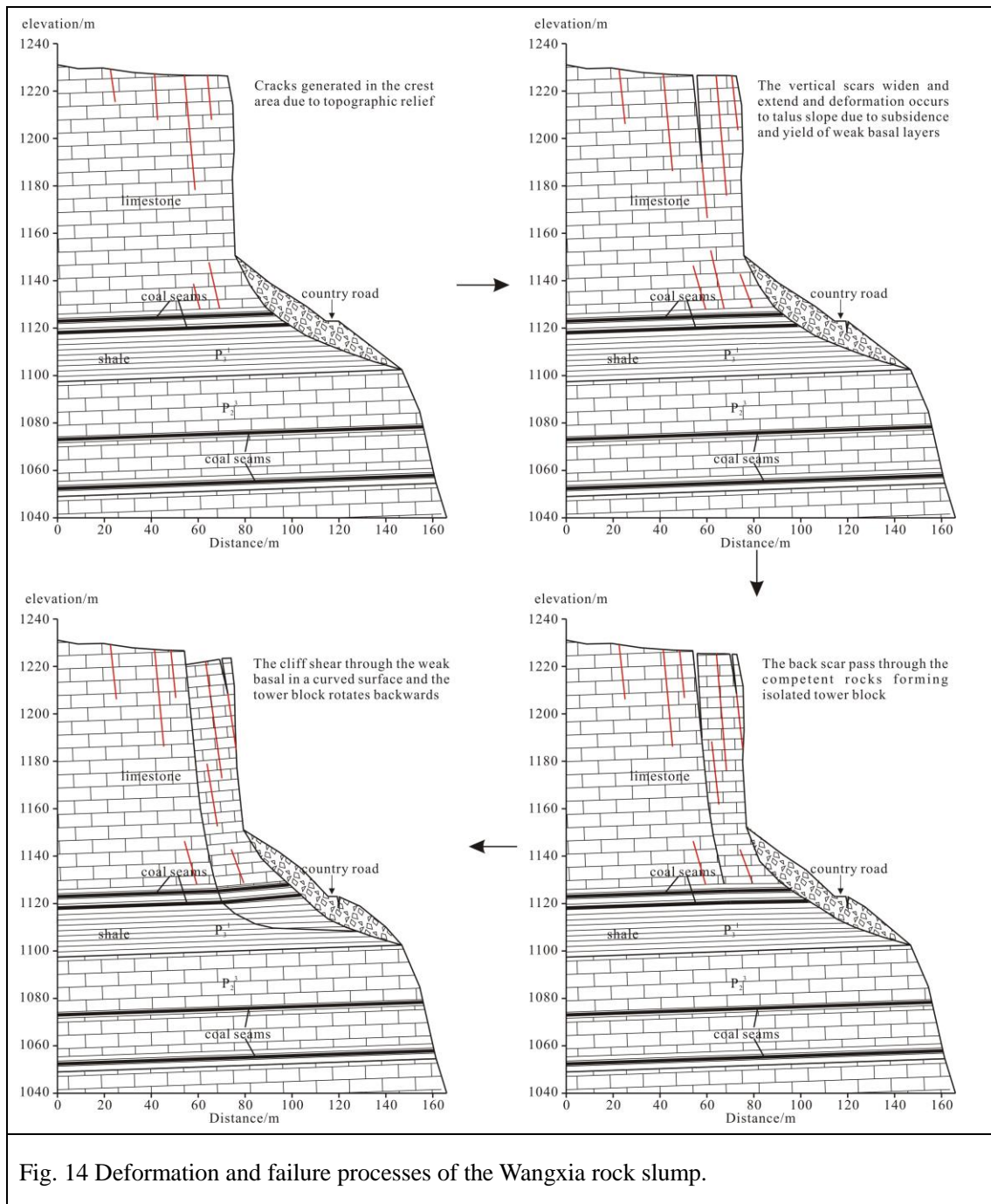


Fig. 14 Deformation and failure processes of the Wangxia rock slump.

241

242 It is worth mentioning that there is a good correlation between the acceleration of displacement  
 243 and concentrated rainfall. Because of cracks and fissures in the limestone, water could easily and  
 244 rapidly percolate into the weak strata. The unconfined compressive strength (UCS) of the shale  
 245 shows a substantial decrease when saturated, and the softening factor is about 0.62. However,  
 246 there is a 2–4 day time lag between concentrated rainfall and acceleration of displacement,

because the infiltration of water into poorly permeable shale takes time.

#### 4. Numerical back-analysis

Numerical analysis is a sophisticated method for assessing the potential failure modes of rock slopes. We use it herein to validate the cases discussed above, which show different failure mechanisms for sub-horizontally bedded cliffs (compound slide, rock collapse, and rock slump) and to explain the backgrounds to the slides. The computation was performed using the computer program UDEC. As discussed, the Yudong rock slide and Wangxia rock slump are characterized by thick shale underlying the cap rock. However, the base of the Zengziyan consists of limestone interbedded with thin shale bands. The calcareous shale in Yudong slide possesses a relatively high strength and the thin shale bands, containing talcum, in Zengziyan collapse is easily weathered and weak. The strength of the carbonaceous shale in Wangxia is moderate comparing to the others. The parameters used in the simulation are given in Table 1.

Table 1 Parameters used in the numerical simulation

parameter	limestone	shale		
		Rock slide	Rock collapse	Rock slump
Thickness (m)	170	20	2	20
Density(kg/m <sup>3</sup> )	2700	2640		
Young's modulus, E(GPa)	65	5		
Poisson'sratio	0.13	0.2		
Friction angle of rock mass ( °)	32	28	20	25
Cohesion of rock mass (MPa)	1.3	0.8	0.4	0.5

Tensile strength of rock mass (MPa)	0.3	0.1	0.04	0.04
Friction angle of joints ( ° )	30	25		
Cohesion of joints (MPa)	1.0	1		
FOS	-	1.01	1.21	1.07

261

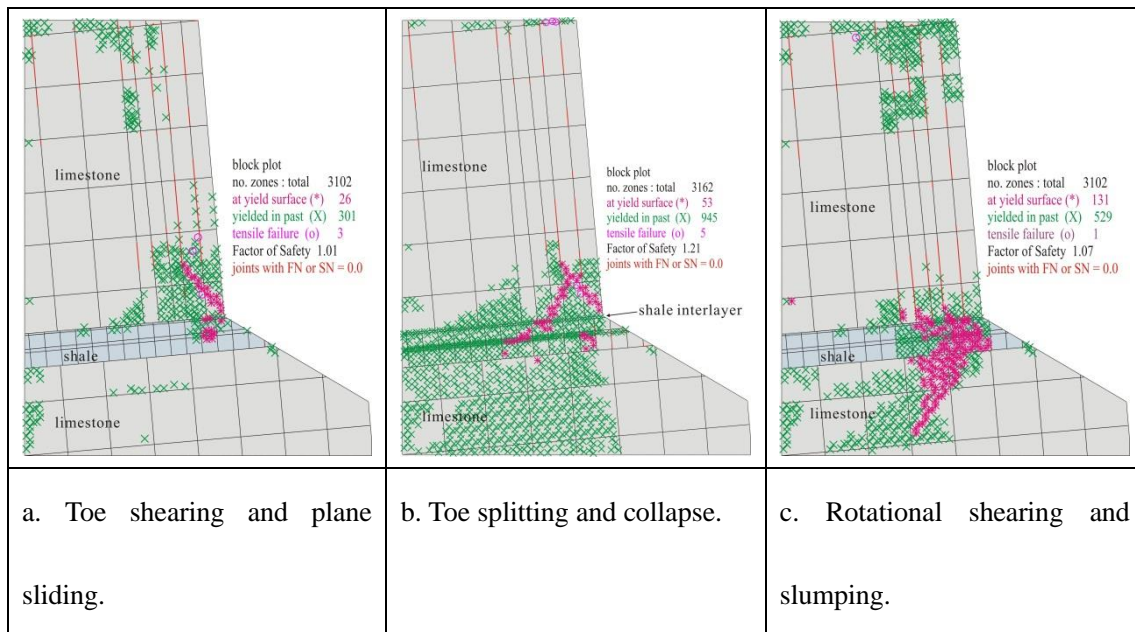


Fig. 15 Plastic state and joint opening for rockslide initiation in cliff slopes.

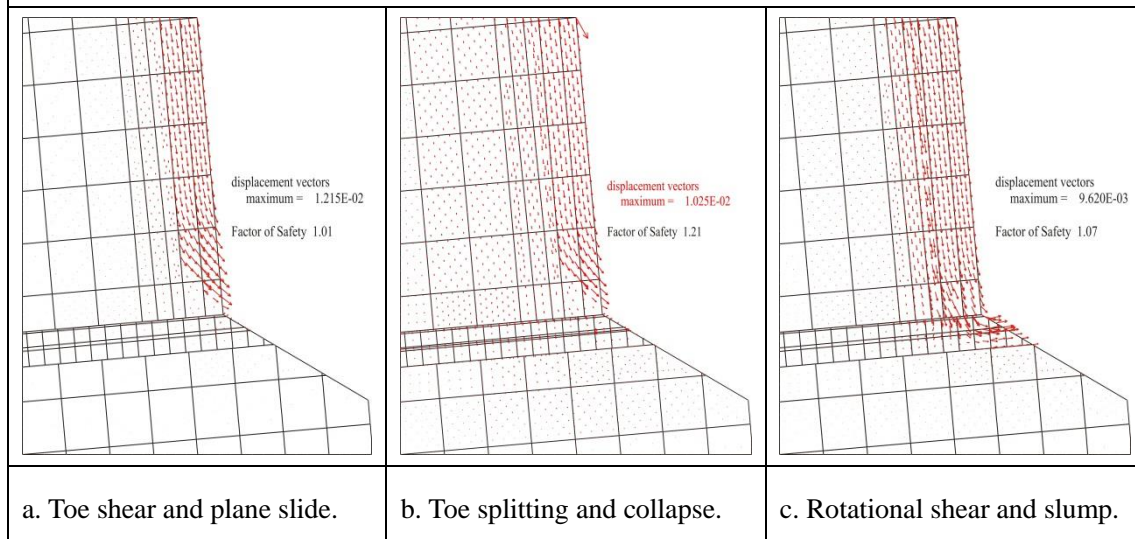


Fig. 16 Displacement vectors of the initial failures of cliff slopes.

262

The natural stress field is characterized by a tensile zone on the crest and stress concentration at the toe. When a thick incompetent basal layers is present, the jointed slope tends to fail as a slump. A yielding curved surface gradually emerges in the basal layers under long-term gravitational compression of the upper cap rock. A large plastic zone is present in the weak basal layers and nearby hard rock mass (Fig. 15c). The horizontal movement of the weak stratum is prominent. Pre-existing joints in the hard rock mass widen upward and slip with the ductile flow of the basal layers. The movement of the massive unstable rock mass is dominated by subsidence in the crest area and back tilting at the toe (Fig. 16c).

When the weak basal is a thin interlayer, rotational slide through the toe is unlikely to occur. The horizontal shear stress determines the possibility of shear failure in the beds. For a sub-horizontal bedded slope with gentle tectonic disturbance during geologic evolution, the horizontal to vertical stress ratio is generally less than 1 (Zhang, et al., 1994). This indicates that it is possible for a weak interlayer with a frictional angle less than  $45^{\circ}$  to shear horizontally. Under these circumstances, the plastic zone ranges over the interlayer as well as the overlying competent rocks. The rock mass at the toe is in a plastic state as a result of compression fractures. Two yield surfaces dipping in opposite directions are formed (Fig. 15b), similar to tensile failure behavior for some brittle rock samples. The displacement prior to collapse is limited, and remarkable squeezing out is unlikely to be observed in the toe area (Fig. 16b).

A rock slide might burst out in hard rock where back scars cut through, and no discontinuities or weak strata are exposed at the toe. Irregular scars caused by brittle and shear failure through rock mass dip out of the cliff faces. The yield zone is mainly located at the block toe but not in the underlying rocks (Fig. 15a). The fracture of the toe rock mass gives rise to joints opening

immediately above. Numerical computation gives a plane yield surface at the bottom of the separated block, which is called a potential failure surface (Fig. 16a). A small displacement appears before the outbreak of a compound slide. However, ground fractures on the crest and spalling in the toe area might occur.

## **5. Underground mining**

The failures at the three locations described above are related to large areas of mining out. Pells (2008) used a 2-D continuum model to assess macro-scale movements of cliff faces caused by total extraction and proved that the steep slope tends to tilt outwards when mining occurs beneath the cliff, and extraction well behind the cliff face causes back tilt. Our similar simulations are shown in Fig. 16. The rock slide model in Fig. 14a was adopted. The roof tends to collapse, and the surrounding rocks gradually fracture. The undermining-induced subsidence of the crest causes the dilation and tensile failure of the rock mass (Fig. 17a). The FOS decreases from 1.01 to 0.98 when the underground mining is located behind the cliff face. When the extraction is directly beneath the cliff, the rock mass is subjected to a small constraint; hence, cliff failure break-out through the fractured rock mass between the goaf and open face is feasible (Fig. 17b). The maximum principal stress on both sides of the goaf increases while that of the overlying rocks decreases (Fig. 17c).

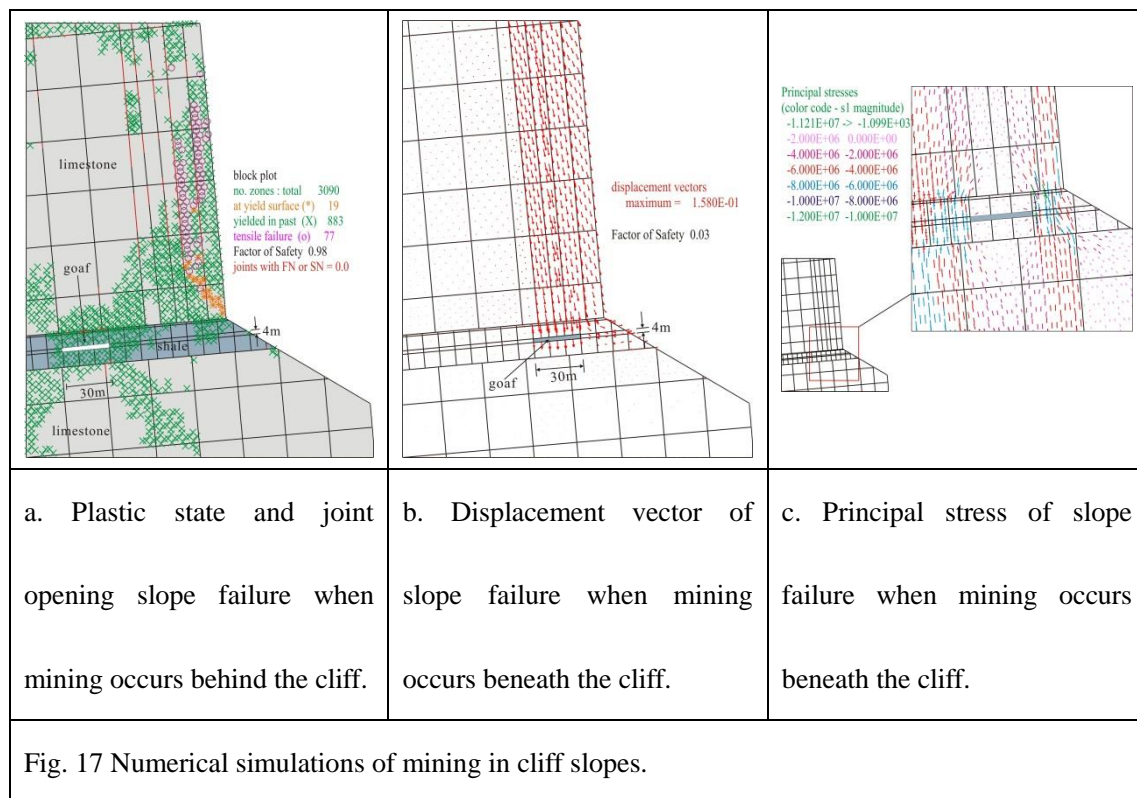


Fig. 17 Numerical simulations of mining in cliff slopes.

## 6. Conclusions

In this study, three different examples of failure in sub-horizontally bedded limestone cliffs are discussed. The failures are characterized by pre-existed vertical joints passing through thick limestone. The Yudong rock slide originated in a limestone cliff edge and left a moderately inclined rupture plane, implying shear failure through the hard rock. Rock collapse caused by compression fracture and tensile splitting of the rock mass near the interface between the hard cap and weak stratum occurred at Zengzi Cliff. The Wangxia cliff failure showed a slow rock slump sheared through the underlying incompetent rock mass along a curved surface. The mechanism of toe breaking mainly depends on the strength characteristics of the rock mass.

Considering that the rock mass near the cliff face is not laterally constrained, it is reasonable to assume that there is a massive UCS failure at the toe of the vertical tower and slab blocks.

Some failure characteristics of jointed rock mass in in situ UCS tests have been observed all



around the world, for both shear and tensile failure. Of special concern is tensile failure in horizontally bedded rock masses with interlayers. Compression fractures emerge near the interfaces and form vertical slabs, which eventually split. Another possibility is squeezing out of weak interlayers as a result of compression fracture, causing the hard rock nearby to yield to tensile stress and disintegrate. It is worth noting that the UCS of the rock mass in compression fracturing is much lower than that of intact rock. A criterion based on horizontal shear failure along weak interlayers and the UCS ratio of the cap and underlying rock masses could be used to assess the failure mode of tower and slab blocks on cliff edges.

#### **Acknowledgments**

This work was carried out with financial support from the China Geological Survey (No. 12120114079101), the Ministry of Science and Technology of the People's Republic of China (No. 2012BAK10B01) and the National Natural Science Foundation of China (No. 41302246).

#### **References**

107 Geology Team of Sichuan Geology and Mineral Bureau. (1995). Geology Survey Report on Bauxite Deposit of Loujiashan in Nanchuan, Sichuan (in Chinese).

Abele, G. (1994). Large rockslides: their causes and movement on internal sliding planes. Mountain Research and Development, 14(4): 315-320.

Altun A.O., Yilmaz I., Yildirim M. (2010). A short review on the surficial impacts of underground mining. Sci Res Essays, 5(21), 3206-3212.

Ding W.W, Yu Y.Z, Deng W.L., et al.(1990). Stability analysis of reservoir bank in Three

338 Gorges of Yangtze River. Center of hydrological and engineering geology, Ministry of Geology  
339 and Mineral Resource, Chengdu: 7-8. (in Chinese)

340 Embleton-Hamann C. (2007). Geomorphological hazards in Austria. Geomorphology for the  
341 Future, Innsbruck University Press, Innsbruck, 33-56.

342 Hungr O., Evans S.G (2004). The occurrence and classification of massive rock slope failure.  
343 Felsbau, 22(2), 16-23.

344 Huang R.Q. (2013). Mechanisms of large-scale landslides and pre-recognition. Key note on  
345 the Six National Academic Conference of Geological Hazard. April 11-12, 2013. Beijing, China.

346 Kay D., Barbato J., Brassington G,et al. (2006). Impacts of Longwall Mining to Rivers and  
347 Cliffs in the Southern Coalfield. In Aziz N. (ed), Coal 2006: Coal Operators' Conference,  
348 University of Wollongong & theAustralasian Institute of Mining and Metallurgy, 2006, 327-336.

349 Le Q.L., Wang H.D., Xue X.Q., et al. (2011). Deformation monitoring and failure mechanism  
350 of Wangxia Dangerous Rock Mass in Wushan County. Journal of Engineering Geology,  
351 19(6):823-830.

352 Li Y., Meng H., Dong Y., Hu S.E. (2004). Main types and characteristics of geo-hazards in  
353 China-based on the results of geo-hazard survey in 209 counties. The Chinese Journal of  
354 Geological Hazards and Control. 15(2):29-34.

355 Lollino P., Martimucci V., Parise M. 2013. Geological survey and numerical modeling of the  
356 potential failure mechanisms of underground caves. Geosystem Engineering, vol. 16 (1): 100-112

357 Marschalko M., Yilmaz I., Bedn árik M., et al. (2012). Deformation of slopes as a cause of  
358 underground mining activities: three case studies from Ostrava–Karvin á coal field (Czech  
359 Republic). Environmental monitoring and assessment, 184(11): 6709-6733.

360 Parise M. (2008) Rock failures in karst. In: Chen ZY, et al (eds) Landslides and Engineered  
361 Slopes. Proc. 10th Int. Symp. on Landslides, Xi'an (China), June 30–July 4, 2008, 1, pp 275-280

362 Parise M. (2010). Hazards in karst. In Proceedings International Interdisciplinary Scientific  
363 Conference “Sustainability of the Karst Environment. Dinaric Karst and Other Karst Regions.”:  
364 Series on Groundwater. IHP-UNESCO, Plitvice Lakes, Croatia (pp. 155-162).

365 Pells P.J.N. (2008). Assessing parameters for computations in rock mechanics. In Potvin Y,  
366 Carter J., Dyskin A., et al (eds), Proceedings First Southern Hemisphere International Rock  
367 Mechanics Symposium (SHIRMS), 1:39-54.

368 Palma B., Parise M., Reichenbach P., et al. 2012. Rock-fall hazard assessment along a road in  
369 the Sorrento Peninsula, Campania, southern Italy. Natural Hazards, 61 (1): 187-201.

370 Rainer P., Martin B., Rudolf H., et al. (2005). Geomechanics of hazardous landslides. Journal  
371 of Mountain Science, 2(3), 211-217.

372 Ren Y.R., Chen P., Zhang J., et al. (2005). Early-warning analysis on the rockfall for  
373 Zengziyan W12# dangerous rock mass in Nanchuan City of Chongqing. The Chinese Journal of  
374 Geological Hazard and Control, 16(2):28-31

375 Rohn J., Resch M., Schneider H., et al. (2004). Large-scale lateral spreading and related mass  
376 movements in the Northern Calcareous Alps. Bulletin of Engineering Geology and the  
377 Environment, 63(1), 71-75.

378 Ruff M., Rohn J. (2008). Susceptibility analysis for slides and rockfall: an example from the  
379 Northern Calcareous Alps (Vorarlberg, Austria). Environmental geology, 55(2), 441-452.

380 Santo A., Del Prete S., Di Crescenzo G., Rotella M. (2007). Karst processes and  
381 slope instability: some investigations in the carbonate Apennine of Campania (southern Italy).

382 In:Parise M, Gunn J (eds) Natural and Anthropogenic Hazards in Karst Areas:  
383 Recognition,Analysis and Mitigation. Geol. Soc. London, sp. publ. 279: 59–72

384 Tang F.Q. (2009). Research on mechanism of mountain landslide due to underground mining.  
385 Journal of Coal Science and Engineering (China), 15(4):351-354.

386 Von Poschinger, A. (2002). Large rockslides in the Alps: A commentary on the contribution  
387 of G. Abele (193 7-1994) and a review of some recent developments. In: Stephen G Evans, et  
388 al.(eds), Catastrophic Landslides: Effects, Occurrence, and Mechanisms,:237-255.

389 White E., White W. (1969). Processes of cavern breakdown. Bull. Natl. Speleol. Soc.  
390 31(4):83–96

391 Zhang C.S., Zhang Y.C., Hu J.J.,Gao Q.Z. (2000). Spatial and temporal distribution  
392 characteristics and forming conditions of Chinese geological disasters. Quaternary Science.  
393 20(6):559-566

394 Zhang Z.Y., Wang S.T., Wang L.S.(1994). Principle of Engineering Geology Analysis. China  
395 Geology Press, Beijing: 66